Synthesis and Spectral Characteristics of Gold Nanoparticles Labelled with Fluorescein Sodium

Article *in* Current Nanoscience · December 2011

DOI: 10.2174/1573413711107061028

2 authors:

Souad A. Elfeky
Cairo University
25 PUBLICATIONS **187** CITATIONS
SEE PROFILE

Alsayed A M Elsherbini
Cairo University
62 PUBLICATIONS **411** CITATIONS
SEE PROFILE

Synthesis and Spectral Characteristics of Gold Nanoparticles Labelled with Fluorescein Sodium

Souad A. Elfeky[a,b,*] and Al-Sayed A. Al-Sherbini[a]

[a]*Department of Laser Applications in Measurements, Photochemistry and Agriculture (LAMPA), National Institute of Laser Enhanced Science (NILES) Cairo University, Cairo, Egypt 12613;* [b]*Department of Chemistry, University of Bath, Claverton down, BA2 7AY, United Kingdom*

Abstract: The biological application of labeled nanoparticles is a rapidly developing area of nanotechnology that raises new possibilities in the diagnosis and treatment of human cancers. Gold nanoparticles (GNPs) have been prepared *via* wet chemical method. Fluorescein capped gold nanoparticles have been prepared by a reduction of the $HAuCl_4$ in boiling fluorescein sodium solution. The results indicated that the spectrum exhibits one curve with two absorption bands at $\lambda_{max.}$= 496, 585 nm, which corresponds to the absorption spectra of both fluorescein and GNPs, respectively. TEM, UV-Visible, fluorescence and IR spectroscopy confirm the formation of GNPs and fluorescein capped GNPs. These fluorescein capped gold nanoparticles can be used in labeling DNA and other imperative biological molecules.

Keywords: Fluorescein sodium, gold nanoparticles, diagnostic, therapeutic and DNA.

1. INTRODUCTION

GNPs are a very important nanomaterial and have been studied extensively due to their unique physical and chemical properties [1-5]. Nanomaterials, which measure 1–1000 nm, allow a unique interaction with biological systems at a molecular level. They can also facilitate vital advances in detection, diagnosis, and treatment of human cancers and have led to a new discipline of nano-oncology [6, 7]. The photothermal properties of GNPs were exploited in therapeutics. GNPs undergo a plasmon resonance with light. This effect can be harnessed to destroy tissue by local heating [8]. One of the main tasks of recent research in diagnostics and cellular imaging is the improvement of highly luminescent biolabelling agents [9-13]. Different types of fluorescent markers have conventionally been used for imaging purposes [9], but organic fluorophores are the most exploited, due to the great number of commercially available molecules that exhibit interesting photophysical features as well as the possibility of tuning such fluorophores for more useful applications. The assemblies of GNPs with dye molecules are attracting more attention [14-16]. An ideal label combines high resolution and easy visualization with minimal perturbation of the properties of the probe to which it is attached. A probe that combines both fluorescent and gold labels is highly enviable. Attempts to prepare such a probe using colloidal gold have resulted in restricted success. It has been found that the loss of fluorescence occurs in preparations including colloidal gold [17, 18]. This might come up from the high extinction coefficient of the colloidal gold particles or from an electronic quenching interaction between the metallic gold and the fluorophore. Huang and Murray have described the quenching of small dyes molecule by gold nanoparticles [19]. While Dubertret and his group have used gold nanoparticles as an effective proximal quencher in DNA molecular beacons [20]. Thus, at present the study on how to chemically modify gold colloid focuses on organic dyes [21]. Fluorescein sodium, resorcinol phthalein sodium or uranine, is the most widely used extrinsic fluorescence probe in bioscience [17]. Its popularity is associated with its long existing history, high extinction coefficient, great fluorescent quantum yield, and well-developed conjugation chemistry to biomolecules. The drawbacks include its inclination to photobleaching, and pH-sensitive fluorescence, although advantages may be taken of the afterward feature to probe local pH values [18]. The spectroscopic characterstics of fluorescein sodium reveal that it absorbs visible light in the blue range with its peak absorption and excitation band occurring at wavelengths between 465-490nm. The fluorescence emission occurs in the yellow-green range from 520 – 530 nm. These fluorescent properties have made fluorescein valuable in a variety and wide range of medical applications [22, 23]. Carboxylate is induced to assemble on the gold nanoparticle surface, so that the nanoparticle with some cations turns into a negatively charged supermolecule, which has specific reaction ability with some cations. For example, they can react with some cationic cellular contents to form a complex nanoparticle by virtue of electrostatic attraction and hydrophobic force. Cationic molecules assemble on the outer layer and wrap the gold nanoparticle, which leads to the changes of spectral characteristics and optical properties [21]. Therefore it can be used in diagnostic and treatment processes. GNPS probes exhibited excellent penetration properties and were used to localize biological target molecules as pre-mRNA splicing factor SC35 in the HeLa cell nucleus by both fluorescence and electron Microscopy [24]. In this study, the fluorescein sodium and the GNPs were integrated into a single compartment. The advantage of this new fluorescein gold probe is that it allows the collection of two complementary sets of data, from fluorescence and from electron microscopy. This advantage could make it valuable for diagnostic and therapeutic applications.

2. EXPERIMENTAL

2.1. Material and Methods

(i) Preparation of Gold Nanospheres

Gold nanospheres were prepared by sodium citrate (puress, Fluka) reduction of the gold salt $HAuCl_4$ (puress, Fluka) according to the following procedure [25]: 1ml of $5x10^{-4}$ mol dm^{-3} $HAuCl_4$ was added to 18 ml double distilled water. The solution was heated until boiling, and then 1ml of 0.5% sodium citrate solution was added, as soon as boiling commenced. The heating of the solution was kept until the color altered from yellow to pale purple. Finally the heating was stopped and the mixture was stirred until it had cooled to room temperature.

*Address correspondence to this author at the Department of Laser Applications in Measurements, Photochemistry and Agriculture. National Institute of Laser Enhanced Science (NILES) Cairo University, Cairo, Egypt 12613; Tel: +447578617765; E-mail: sae21@bath.ac.uk

1573-4137/11 $58.00+.00

(ii) Preparation of Fluorescein Sodium-Coated Gold Nanoparticles

Fluorescein sodium-coated GNPs were prepared as follows: $1x10^{-3}$ mol dm^{-3} of fluorescein sodium (uranine) puriss (FLUKA) was dissolved in double distilled water. The solution was degassed for at least 10 mins by nitrogen in order to avoid oxidation. The solution was allowed to boil under vigorous stirring. Then, 20 ml of $5x10^{-3}$ mol dm^{-3} $HAuCl_4$ was added dropwise whilst boiling. The color of the mixture changed from bright yellow-green to orange red. The mixture was further allowed to boil for additional 15 min. After cooling to room temperature the nanoparticles were separated by the centrifugation method at 6000 rpm for 20 minutes. The blue precipitate was collected and washed three times with double distilled water for further spectroscopic characterization.

2.2. Instrumentation

The electronic UV-visible absorption spectra were recorded on a *Perkin Elmer lambda-17* spectrophotometer, using a quartz cell with a pathlength of 1 cm. The fluorescence spectra measurements were conducted on a *Shimadzu RF-5000* luminescence spectrometer, using a quartz cell and a 1 cm cuvette holder. Fluorescence intensities were measured at right angles to the exciting light. The slit width was a narrow entrance in order to minimize the intensity of the exciting light. All measurements were carried out at room temperature. The shape and size of the obtained particles have been determined by Transmission Electron Microscopy (TEM). One drop of the sample solution was dried on a carbon-coated copper TEM grid. Particles sizes were determined from the micrographs of the Joel-100S transmission electron microscope operating at 120 KV. Fourier-transformed infrared (FT-IR) spectra were measured on a *Perkin Elmer-200*0 FT-IR system (*Perkin Elmer*, Norwalk, CT) using the KBr disk method (2 mg sample in 200 mg KBr). The scanning range was 450 to 4000 cm and the resolution was 1 cm.

3. RESULTS AND DISCUSSION

3.1. The Spectral Characteristics of Gold Nanoparticle-Fluorescein System

(i) Absorption Spectra

GNPs show a strong light absorption in the visible region at λ_{max} 526 nm (Fig. (**1**)). This strong absorption results from nanoparticles' coherent oscillation of the free electrons on the particle surface (surface plasmon resonance) [25, 26].

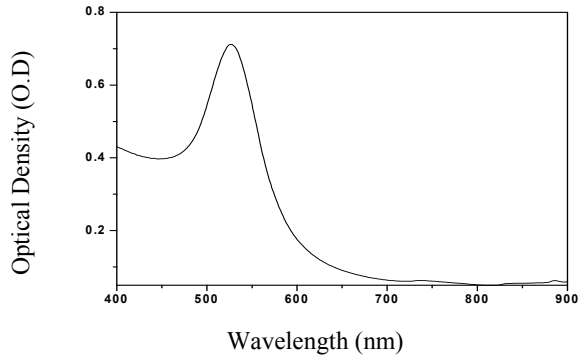

Fig. (1). UV-visible spectra of $3x10^{-5}$ mol dm^{-3} spherical GNPs prepared by citrate reduction method.

Comparison of the UV/visible spectrum of the unattached fluorescein, and fluorescein-Nanogold was found to be additive. Fig. (**2-a, b**) shows the absorption spectra of both the unattached fluorescein ($1.3x10^{-5}$ mol dm^{-3}) and the fluorescein-Nanogold respectively.

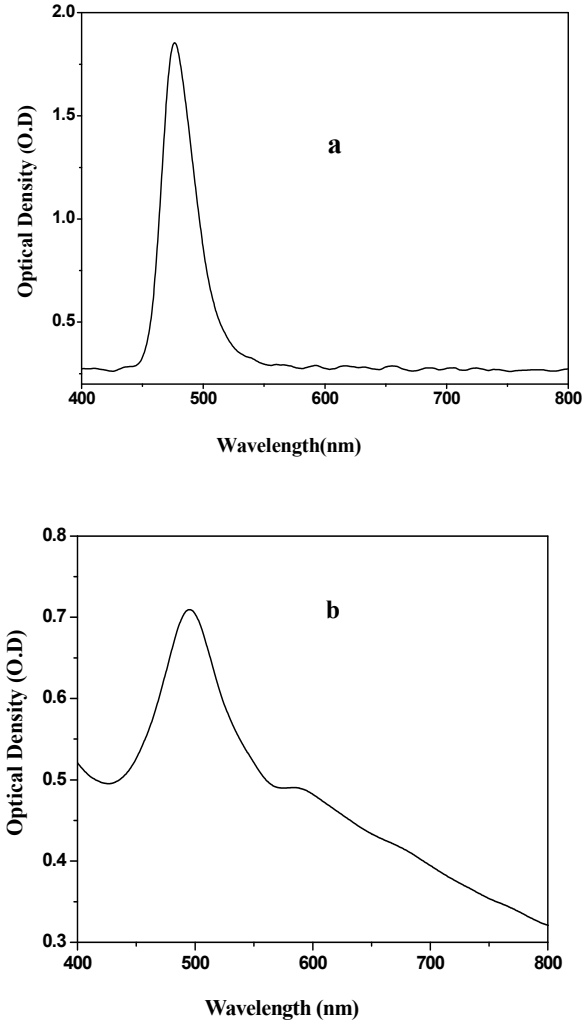

Fig. (2). a-The absorption spectra of 1.3×10^{-5} mol dm^{-3} fluorescein sodium, **b**-The absorption spectra of fluorescein-coated GNPs.

Fig. (**2-a**) The absorption spectrum exhibits a single absorption band in the visible region at λ_{max} 476 nm arising from one resonance system of the whole molecule, i.e. involving an intramolecular charge transfer interaction as depicted in Scheme **1**.

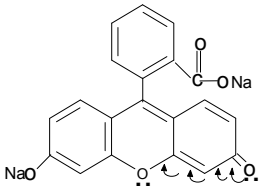

Scheme 1. Fluorescein sodium

In Fig. (**2b**) fluorescein-coated GNPs exhibit two absorption bands arising from each component of fluorescein-Nanogold. The two bands are obviously red shifted with significant broadness. The first band at λ_{max} 496 nm corresponds to the absorption spectra of fluorescein with bathochromic shift ($\Delta\lambda$) about 20 nm. The second absorption band at λ_{max} 580 nm relates to GNPs with bathochromic

shift (Δλ) about 54 nm. Observations similar to these were reported by Norris & Meisel and co-workers [27]. It can be seen that when GNPs combine with fluorescein, the solution changes from wine red to blue and the absorption peak red shifts to 580 nm. Therefore it can be concluded that the combination of gold nanoparticle with fluorescein results in a new absorption spectrum which differs from that of the gold nanoparticle and fluorescein separately [21]. The noticed peak broadness of fluorescein due to the attachment of fluorescein to GNPs may result from the change in electron density of fluorescein caused by removal of sodium cation and binding to nanogold. Now, the overall electron density in the fluorescein dye contributes to the spectral broadening characteristics of the gold nanoparticle-fluorescein system. Furthermore, fluorescein-Nanogold binding-induced aggregation of spherical particles is due to the greater electrostatic attraction of the dye with GNPs. The concept here is that, when the separation distance between particles is comparable to or smaller than their radii, the oscillation of the plasmons from adjacent particles can become coupled, lowering their vibration frequency that appear as absorption bands red-shifted to longer wavelengths. The red-shift is dependent upon the number of particles and their spatial arrangement within the aggregate [28, 29].

(ii) Fluorescence Spectra

It was found by Meisel and his coworkers [30] that the characteristics and position of absorption and emission band maximum depend largely on the particle diameter, medium and surface absorption species. Fluorescence emission of both fluorescein and fluorescein-coated GNPs was measured at $\lambda_{ex.}$= 470 nm (Fig. (**3a, b**)).

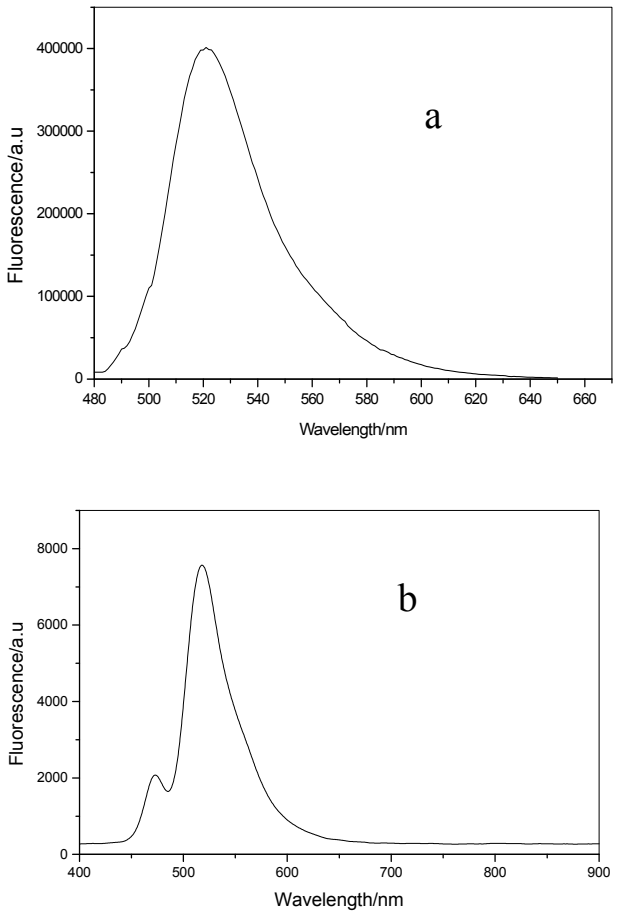

Fig. (3). a-Fluorescence emission spectra of fluorescein sodium, **b**- Fluorescence emission spectra of fluoresein-coated GNPs at $\lambda_{ex.}$= 470 nm.

Fig. (**3a**) displays fluorescence spectra of unbound fluorescein sodium (1.3×10^{-5} mol dm^{-3}) aqueous solution. The spectrum in Fig. (**3b**) represents the quenched fluorescence spectrum of the composite system (sketched in Scheme **2**) due to the reabsorption of molecular fluorescence light by GNPs as well as the near field effects on the absorption cross section [31]. This reabsorption effect is clarified in Fig. (**4**) which shows the correspondence between GNPs absorption and fluorescein emission.

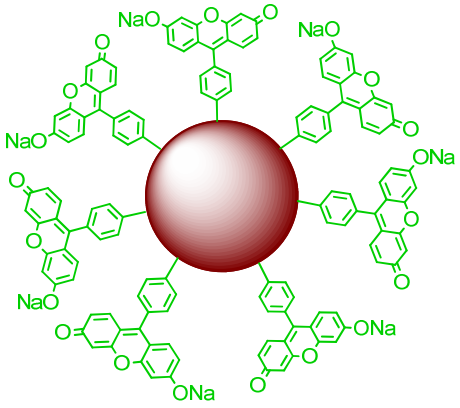

Scheme 2. Fluorescein sodium assembled on the gold nanoparticle surface in a composite system.

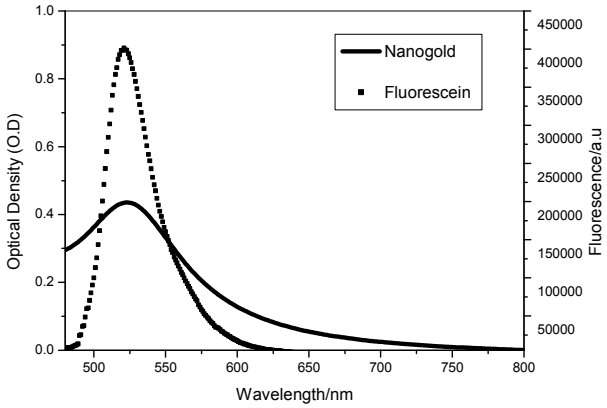

Fig. (4). Absorption spectrum of a gold nanoparticle solution (solid curve) and fluorescence spectrum of fluorescein sodium (1.3×10^{-5} mol dm^{-3}) aqueous solution (dotted curve) at λ_{ex}=470 nm.

This reabsorption is attributed to the resonance energy transfer from fluorescein to GNPs [32-34]. The probability of this Forster energy transfer depends on the overlap of the fluorescence band of dye molecule with the absorption band of the acceptor. In the present case, fluorescein fluorescence band at 520 nm overlaps with the surface plasmon band of GNPs at 526 nm and one expects effective energy transfer from the excited fluorescein molecules to the gold surface [27]. Furthermore, the smaller gold nanoparticles are more efficient quenchers due to their larger surface areas. Images of fluorescein and fluorescein-capped GNPs (Fig. (**5**)) were taken under irradiation of UV lamp.

In Fig. (**5a**) the irradiation of fluorescein sodium and fluorescein-GNPs by UV-light shows a strong luminescence emission of fluorescein sodium (left) while the emission was dramatically quenched after binding to GNPs (right) at pH=7.5. Fig. (**5b**) demonstrates a strong emission for both fluorescein sodium (left) and fluorescein-modified GNPs (right) after irradiation to UV-light in alkaline media (pH=9). This is because fluorescein can be reversi-

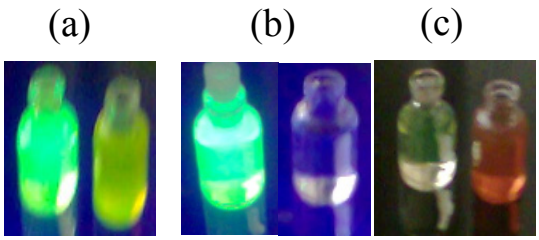

Fig. (5). (**a**, **b**): Fluorescein sodium and fluorescein-modified GNPs under irradiation with UV lamp, (**c**) Without UV irradiation.

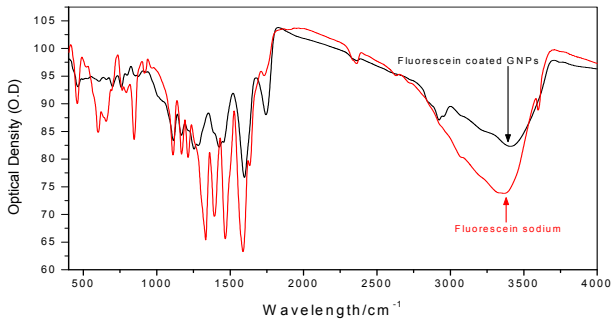

Fig. (6). FT-IR spectra of Fluorescein sodium (1.3×10^{-5} mol dm^{-3}) and the synthesized fluorescein-coated GNPs.

bly chemisorbed onto colloidal gold particle surfaces. It can be released from the surface without any significant change in its intrinsic optical properties at an alkaline pH. In other words, there is electrostatic repulsion between the negatively charged particles at alkaline pH [27]. Fig. (**5c**) shows no emission for each of fluorescein sodium (left) and fluorescein-modified GNPs (right) at pH 9 without UV irradiation.

(iii) IR Spectra

Additional information from infrared spectroscopy is useful.

Fig. (**6**) shows the FT-IR spectra of fluorescein sodium in pure form and the synthesized fluorescein-coated GNPs. The variations in the band intensities reflect molecular structure change [35]. It can be seen that the IR pattern of the fluorescein is appreciably modified by binding to GNPs surface. For example, the intensity of absorption bands of fluorescein-coated GNPs is weaker than that of fluorescein sodium Table **1**.

In Table **1** the vibration at 1105 cm^{-1} is mainly due to asymmetric CCH bend and the vibrational band at 1167cm^{-1} involve considerably CCH bends on the xanthene ring. The band at 1213 cm^{-1} involves COC stretch and bend, and CCH bend as well. According to Davies and Jones, the band at 1213 cm^{-1} is due to the absorption of the ether linkage, C-O-C [36]. The interpretation of the data in the region around 1333 cm^{-1} most likely result from xanthene CC stretch. Davies and Jones, however, stated the vibrational bands at 1398 cm^{-1} (fluorescein sodium) as the symmetric carboxylate stretch based on the observation of the symmetric carboxylate stretch at 1411 cm^{-1} in sodium benzoate and at 1418 cm^{-1} in sodium acetate [39]. The disappear of the band at 1398 cm^{-1} in case of fluorescein-coated GNPs indicates that the adsorption of fluorescein on gold occurs at this position to form the corresponding fluorescein-coated GNPs as illustrated in Scheme **2**. The IR band of fluorescein sodium involving asymmetric carboxylate stretch at 1587 cm^{-1} was reported consistently in literature [36, 39, 40]. The result of the asymmetric stretch at 1587 cm^{-1} is consistent with those reports on IR spectra of solid fluorescein [36, 39, 40]. In two reports [36, 40], the band at 1467 cm^{-1} was assigned to the symmetric carboxylate stretch. Hildebrandt and Stockburger reported the three stretching vibrations of xanthene ring at 1324, 1548, and 1629

Table 1. The Vibrational Bands (in cm^{-1}) Observed in FTIR Spectra of Fluorescein and Fluorescein-Coated GNPs in Aqueous Solutions and their Assignments Based on Literature

Fluoresein	Fluorescein-Coated GNPs	Assignments [Literature]
1105	1105 w	Aromatic C-H [36, 37]
1167	1167 w	C-OH (phenolic) [36,38]
1213	1213 w	C-O-C stretch of XR [39]
1333	1260 w	Phenoxide ion stretch conjugated with CCH bend, CC stretch and C-O XR stretch [39]
1398		(a) Aromatic skeletal C-C stretch [40], (b) symmetric COO^- stretch [39]
1467	1420 w	(a) XR skeletal C-C stretch conjugated with symmetric COO^- stretch [37], (b) symmetric COO^- stretch [36]
1587		(a) XR skeletal C-C stretch containing conjugated carbonyl band and asymmetric carboxylate stretch [40], (b) asymmetric COO^- stretch [39,36]
	1597 w	XR skeletal C-C stretch containing conjugated carbonyl band [39]
1731 w	1743	very symmetric CO and CC stretch
3356	3415	O-Na stretch

W refer to weak

XR is abbreviation of the xanthene ring

The interpretations of some vibrational bands were somewhat different in various literatures. We labeled them as (a) and (b).

cm^{-1} by means of Surface Enhanced Resonance Raman measurements of fluorescein adsorbed on colloidal silver [41]. We reported three stretching vibrations of xanthene ring at 1420, 1597, and 1743 cm^{-1} by means of FT-IR measurements of fluorescein adsorbed on colloidal gold. The FTIR spectra of fluoresein-coated GNPs and fluorescein sodium show broad bands centred at 3415 and 3356 cm^{-1} respectively attributable to the phenolic O-Na stretching frequency.

3.2. The Shape and Diameter of GNPs and the Product Fluorescein-Nanogold

The shape and diameter of the GNPs and the complex resulting from the combination of GNPs with fluorescein have been observed with TEM. The results are shown in Fig. (**7**).

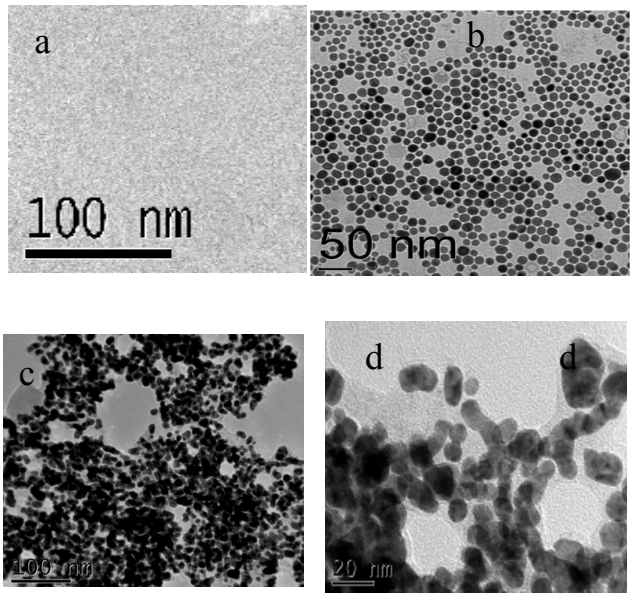

Fig. (7). TEM micrographs of a- Fluorescein sodium, b- GNPs, c- functionalized fluorescent GNPs-fluorescein system, and d- functionalized fluorescent GNPs- fluorescein system at high magnification.

Fig. (**7a**) illustrates the fluorescein dye molecules only with no detectable size. In Fig. (**7b**) it can be seen that the red GNPs are homogenous, dispersed and almost spherically-shaped. The average diameter is about 10 ±0.5 nm, which is consistent with reference [42]. When it interacts with fluorescein to form a blue product, fluorescein assembles on the surface of gold nanoparticle, which results in the increase in the diameter to approximately 15 nm ± 0.5 nm [42], Figs. (**7c**&**d**). The product is also spherically-shaped; therefore the assembly of dye on the GNPs surface leads to the increase in the size of the nanoparticle, but barely affects the shape of the nanoparticle [21].

4. CONCLUSION

This is the first time fluorescein labelled nanogold has been prepared. The anchoring of fluorescein to GNPs is remarked by fluorescence quenching. The shape and diameter of GNPs and the complex of GNPs with fluorescein have been examined with TEM. This new fluorescent probe should be useful for a variety of applications in biological microscopy.

ACKNOWLEDGMENTS

This work has been supported by National Institute of Laser Enhanced Sciences (NILES) Cairo University-Egypt.

REFERENCES

[1] Mohamed, M. B.; Ahmadi, T. S.; Link, S; Braun, M.; El-Sayed, M. A. Hot electron and phonon dynamics of gold nanoparticles embedded in a gel matrix. *Chem. Phys. Lett*. **2001**, *343*, 55-63.

[2] Feldsteon, M. J.; Keating, C. D.; Liau, Y. H.; Natan, M. J.; Scherer, N. F. Electronic relaxation dynamics in coupled metal nanoparticles. *J. Am. Chem. Soc*. **1997**, *119*, 6638-6647.

[3] Grabra, K. C.; Freeman, R. G.; Hommer, M. B.; Natan, M. J. Preparation and characterization of Au colloid monolayers. *Anal. Chem.* **1995,** *67*, 735-743.

[4] Garcia, M. E.; Baker, L. A.; Crooks, R. M. Preparation and characterization of dendrimer-gold colloid nanocomposites. *Anal. Chem*. **1999**, *71*, 256-258.

[5] Storhoff, J. J.; Lazarides, A. A.; Mucic, R. C.; Mirkin, C. A.; Letsinger, R. L.; Schatz, G. C. What controls the optical properties of DNA -linked gold nanoparticle assemblies? *J. Am. Chem. Soc*. **2000**, *112*, 4640-4650.

[6] Jain, K. Nanotechnology in clinical laboratory diagnostics. *Clin. Chim. Acta* **2005**, *358*, 37-54.

[7] Ferrari, M. Cancer nanotechnology: opportunities and challenges. *Nat. Rev. Cancer* **2005**, *5*, 161-171.

[8] Pissuwan, D.; Valenzuela, S. M.; Cortie, M. B. Therapeutic possibilities of plasmonically heated gold nanoparticles. *Trends Biotechnol.*, **2006**, *24*(2), 62-67.

[9] Miletto, I.; Gilardino, A.; Zamburlin, P.; Dalmazzo, S.; Lovisolo, D.; Caputo, G.; Viscardi, G.; Martra, G. Highly bright and photostable cyanine dye-doped silica nanoparticles for optical imaging: Photophysical characterization and cell tests. *Dyes Pigm.* **2010**, *84*, 121-127.

[10] Sharma, P.; Brown, S.; Walter, G.; Santra, S.; Moudgil, B. Nanoparticles for bioimaging. *Adv. Colloid Interface Sci*. **2006**, *123-126*, 471-485.

[11] Medintz, I. L.; Tetsuo, U. H.; Goldman, E. R.; Mattoussi, H. Quantum dot bioconjugates for imaging, labelling and sensing. *Nat. Mater.*, **2005**, *4*(6), 435-446.

[12] Michalet, X.; Pinaud, F. F.; Bentolila, L. A.; Tsay, J.M.; Doose, S.; Li, J.J.; Sundaresan, G.; Wu, A.M.; Gambhir. S. S.; Weiss, S. Quantum dots for live cells *in vivo* imaging and diagnostics. *Science*, **2005**, *307*(5709), 538-544.

[13] Wang, L.; Zhao, W.; Tan, W. Bioconjugated silica nanoparticles: development and applications. *Nano Res*. **2008**, *1*(2), 99-115.

[14] Marcel, B. J.; Mario, M.; Peter, G.; Shimon, W.; Paul, A. Semiconductor nanocrystals as fluorescent biological labels. *Science*, **1998**, *281*, 2013-2015.

[15] Nasr, C.; Liu, D.; Hotchandani, S.; Kamat, P. Dye-capped semiconductor nanoparticles, excited state and photosensitization aspects of rhodamine 6G-aggregates bond to SiO_2 and SnO_2 colloids. *J. Phys. Chem*. **1996**, *100*(26), 11054-11061.

[16] Chandrasekharan, N.; Kamat, P. Dye-capped gold nanoclusters: Photoinduced morphological changes in gold/rhodamine 6G nanoassemblies. *J. Phys. Chem. B*. **2000**, *104*(47), 11103-11109.

[17] Goodman, S. L.; Park, K.; Albrecht, R. M. A correlative approach to colloidal gold labelling with video-enhanced light microscopy, low-voltage scanning electron microscopy, and high-voltage electron microscopy. In Hayat, M.A; Ed. Colloidal Gold: Principles, Methods and Applications.; Academic Press: San Diego, **1991**; Vol. *3*; p. 369.

[18] De Brabander, M.; Geuens, G.; Nuydens, R.; Moeremans, M.; De Mey, J. Probing microtubule-dependent intracellular motility with nanometre particle video ultramicroscopy (nanovid ultramicroscopy). *Cytobios*, **1985,** *43*, 273-283.

[19] Huang, T.; Murray, R. W. Quenching of $[Ru(bpy)^3]^{2+}$ Fluorescence by Binding to Au Nanoparticles. *Langmuir*, **2002**, *18*, 7077-7081.

[20] Dubertret, C.; Gorwood, P.; Gouya, L.; Deybach, J. C.; Ades, J. Association and excess of transmission of a DRD2 haplotype in a sample of French schizophrenic patients. *Schizophr. Res*. **2001**, *49*, 203-212.

[21] Youqiu, H.; Shaopu, L.; Qin, L.; Zhongfang, L.; Xiaoli, H. Absorption, fluorescence and resonance Rayleigh scattering spectral characteristics of interaction of gold nanoparticle with safranine T. *Sci. Chin. Ser. B,* **2005**, *48*(3), 216-226.

[22] Valentin, B.; Stefan, D.; Monther, B.; Artemisia, K.; Roland, M.; Alexander, M. Intravenous application of fluorescein for confocal laser scanning microscopy: evaluation of contrast dynamics and image quality with increasing injection-to-imaging time. *Gastrointest. Endosc*. **2008**, *68*(2), 319-323.

[23] Xun, L.; William, M.; Frank, T.; Zbigniew, D. Application of Biotin, Digoxigenin or Fluorescein Conjugated Deoxynucleotides to Label DNA Strand Breaks for Analysis of Cell Proliferation and Apoptosis Using Flow Cytometry. *Biotech. Histochem*. **1995**, *70*(5), 234-242.

[24] Richard, D. P.; Carol, M. R.; David, L. S.; Shelley, L. K.; Jennifer, M.; James, F. H. A Covalent Fluorescent–Gold Immunoprobe: Simultaneous Detection of a Pre-mRNA Splicing Factor by Light and Electron Microscopy. *J. Histochem. Cytochem.* **1997**, *45*, 947-956.

[25] Link, S.; El-Sayed, M. Shape and size dependence of radiative, non-radiative and photothermal properties of gold nanocrystals. *Int. Rev. Phys. Chem.* **2000**, *19*(3), 409-453.

[26] El-Sayed, M. Some Interesting Properties of Metals Confined in Time and Nanometer Space of Different Shapes. *Accounts Chem. Res.* **2003**, *34*, 4.

[27] Olga, V. M.; Agnes E. O.; Hirokazu M.; James, R. N.; Meisel, D.; Adsorption and Encapsulation of Fluorescent Probes in Nanoparticles. *J. Phys. Chem. B.* **1999**, *103*, 9080-9084.

[28] Quinten, M.; Kreibig, U. Optical properties of small metal particles. *Surf. Sci.* **1986**, *172*, 557-577.

[29] Tom, R.T.; Suryanarayanan, V.; Reddy, P. G.; Baskaran, S.; Pradeep, T. Ciprofloxacin protected gold nanoparticles. *Langmuir*, **2004**, *20*, 1909.

[30] Mulvaney, P. I.; Kamat, P. V.; Meisel, D. *Semiconductor Nanoclusters-Physical, Chemical and Catalytic Aspects*. Elsevier Science*:* Amsterdam, **1997**; 99-123.

[31] Jian, Z.; Jian-jun, L.; A-qing, W.; Yu, C.; Jun-wu, Z. Fluorescence Quenching of Alpha-Fetoprotein by Gold Nanoparticles: Effect of Dielectric Shell on Non-Radiative Decay. *Nanoscale Res. Lett.* **2010**, *5*, 1496-1501.

[32] Dulkeith, E.; Morteani, A. C.; Niedereichholz, T.; Klar, T. A.; Feldmann, J. Fluorescence Quenching of Dye Molecules near Gold Nanoparticles: Radiative and Nonradiative Effects. *Phys. Rev. Lett.* **2002**, *89*, 20.

[33] Whitmore, P. M.; Robota, H. J.; Harris, C. B. Mechanisms for electronic energy transfer between molecules and metal surfaces: A comparison of silver and nickel. *J. Chem. Phys.* **1982**, *77*(3), 1560.

[34] Waldeck, D. H.; Alivisatos, A. P.; Harris, C. B. Nonradiative damping of molecular electronic excited-states by metal-surfaces. *Surf. Sci.* **1985**, *158*, 103.

[35] Wang, L.; Roitberg, A.; Meuse, C.; Gaigalas, A. Raman and FTIR spectroscopies of fluorescein in solutions. *Spectrochim. Acta A*, **2001**, *57*, 1781-1791.

[36] Issa, I.; Issa, R.; Temerk, Y.; Ghoneim, M. The infrared spectra of fluorescein and some of its halogen derivatives. *Egypt. J. Chem*, **1974**, *17*, 391.

[37] Colthup, N.; Daly, L. Wiberley, S. Introduction to Infrared and Raman Spectroscopy. *3rd Ed.*, Academic Press: San Diego, **1990**.

[38] Lin-Vien, D. Colthup, N. Fateley, W. Grasselli, J. *The Handbook of Infrared and Raman Characteristic Frequencies of Organic Molecules*, Academic Press: San Diego, **1991**.

[39] Davies, M. Jones, R. The infrared absorptions of fluorescein and some alkali derivatives. *J. Chem. Soc.*, **1954**, 120.

[40] Markuszewski, R.; Diehl, H. The infra red spectra and structures of the three solid forms of fluorescein and related compounds. *Talanta*, **1980**, *27*, 937.

[41] Hildebrandt, P.; Stockburger, M. Surface enhanced resonance Raman study on fluorescein dyes. *J. Raman Spectrosc.*, **1986**, *17*, 55-58.

[42] Zhao, H. Q.; Lin, L.; Tang, J. A. Using gold nanoparticles enhance fixity and discernable ability of DNA probe on sensor. *Chin. Sci. Bull.* **2001**, *46*(4), 292-294.

Received: April 01, 2011 **Revised: May 31, 2011** **Accepted: September 05, 2011**